

JAERI-M

8938

SOME CONSIDERATIONS OF DESIGN
ISSUES ON TOROIDAL FIELD
RIPPLE

June 1980

Tatsuzo TONE, Takashi YAMAMOTO*, Keiji TANI,
Masayoshi SUGIHARA and Masao KASAI**

この報告書は、日本原子力研究所が JAERI-M レポートとして、不定期に刊行している研究報告書です。入手、複製などのお問い合わせは、日本原子力研究所技術情報部（茨城県那珂郡東海村）あて、お申しこしてください。

JAERI-M reports, issued irregularly, describe the results of research works carried out in JAERI. Inquiries about the availability of reports and their reproduction should be addressed to Division of Technical Information, Japan Atomic Energy Research Institute, Tokai-mura, Naka-gun, Ibaraki-ken, Japan.

Some Considerations of Design Issues
on Toroidal Field Ripple

Tatsuzo TONE, Takashi YAMAMOTO^{*}, Keiji TANI,
Masayoshi SUGIHARA and Masao KASAI^{**}

Fusion Research and Development Center
Tokai Research Establishment, JAERI

(Received June 11, 1980)

This report describes the effect of toroidal field ripple on the injected beam ion confinement and the ripple level required for stable burning for the INTOR plasma. The confinement of beam ions is analyzed with a Monte Carlo orbit-following calculation code and the burn control is simulated with a one-dimensional transport code. The results obtained are discussed from the viewpoint of related engineering design issues.

Keywords: INTOR, Tokamak Reactor, Toroidal Field Ripple, Neutral Beam,
Burn Control, Monte Carlo Calculation, One-Dimensional Transport

* On leave from Fuji Electric Co. Ltd., Kawasaki, Japan

** On leave from Mitsubishi Atomic Power Industries Inc., Omiya, Japan

トロイダル・フィールド・リップルに関わる設計課題の考察

日本原子力研究所東海研究所核融合開発推進センター

東稔 達三・山本 孝^{*}・谷 啓二
杉原 正芳・笠井 稚夫^{**}

(1980年6月11日受理)

トカマク・プラズマ中にトロイダルコイルによって生じるフィールド・リップルは、プラズマイオンのエネルギー輸送、加熱のために入射された高速イオンの閉込め、DT反応で生じた高エネルギーアルファ粒子の閉込め等に影響を及ぼす。このリップルの問題を工学設計の立場からみると、トロイダルコイルの数と大きさ、ポロイダルコイルの配位、電源の大きさ、中性粒子入射加熱装置の設置角度、燃焼制御用コイルの設置、トロイダルコイル内側の必要空間（遮蔽、ブランケット、分解修理等）、及び入射粒子による第1壁の局部加熱等が関連してくる。

このレポートでは、INTORトカマク炉を対象としてもっとも主要な物理現象である入射高速粒子の閉込めとリップルによる燃焼制御について、それぞれモンテカルロ軌道計算コードと1次元輸送コードによって広範囲に解析を行った。これらの結果に基づいて、関連する工学的諸問題の議論を行っている。

なお、このレポートは6月16～27日のINTORワークショップにおける設計パラメータの選定のための資料として作成されたものである。

* 外来研究員；富士電機製造（株）

** 外来研究員；三菱原子力工業（株）

CONTENTS

1. Introduction	1
2. Toroidal field ripple	2
3. Ripple loss of fast ions during slowing down	3
3.1 Model	3
3.2 Results	4
4. Toroidal field ripple required to achieve a stable plasma burning	7
5. Discussion	10
Acknowledgement	11
References	12

目 次

1. 序	1
2. トロイダルフィールド・リップル	2
3. 高エネルギーイオンの減速中の損失	3
3.1 モデル	3
3.2 結果	4
4. 安定した燃焼の達成のために必要なリップル	7
5. 議 論	10
謝 辞	11
文 献	12

1. Introduction

Toroidal field ripple brings about some disadvantages in a tokamak plasma, though it may be useful for active burn control. The disadvantages considered are enhanced ion thermal transport in a collisionless plasma, deteriorated confinement of perpendicularly injected beam ions and of banana-trapped alpha particles, etc. The effect on ion thermal transport will prevent ignition, and the deterioration of the beam ion confinement requires a larger injection power and special measures for protection against local heat load on the first wall. The effect on the alpha-particle confinement is not significant. In connection with the acceptable ripple the determination of the number and size of toroidal field coils is greatly influenced.

For the INTOR plasma⁽¹⁾ we have taken up the two major issues on field ripple in this report: (1) effect on beam ion confinement, (2) ripple required for stable burning. The confinement of injected beam ions during slowing down has been analyzed with a Monte Carlo orbit-following calculation code⁽²⁾. The two kinds of loss processes, ripple-trapped drift loss and banana drift loss, have been simulated and the heat load on the first wall has been estimated. The influence of the number of TF coils on the energy loss of beam ions is surveyed.

The simulation of the NBI heating phase to ignite the INTOR plasma and of stable burning has been performed with a one-dimensional transport code⁽³⁾. The empirical scaling law is used for electron energy confinement. The ion thermal conductivity is given by a 3 times enhancement over the neoclassical value.

2. Toroidal field ripple

The toroidal field ripple has been calculated based on constant tension D-shaped coils. All the calculations are made with the center of the inboard leg set at $R_1 = 2.25$ m in the midplane. The value of R_1 is chosen with reference to INTOR-J⁽⁴⁾.

Figure 1 shows ripple values at the outer edge of the plasma for 8~16 coils as a function of the radius R_2 at the center of the outboard leg. The ripple is defined by Eq.(2) in the next section. The upper limit of acceptable ripple imposed by INTOR Group⁽¹⁾, 0.75 %, is marked in the figure. In case of 12 coils, for example, R_2 for the 0.75 % ripple is 10 m. We see in the figure that as the number (N) of TF coils decreases the increasing rate of R_2 becomes large.

Figure 2 illustrates the cross section of toroidal field coils as viewed from above, for 0.75 % ripple at the outer edge of the plasma. The figure for 12 coils is depicted with reference to INTOR-J. The points A and B marked on the shield side represent round corners where the straight shield line (\overline{AB}) is bended. The angle of 16° shown in the figure is made between the straight line \overline{AB} and the normal to the plasma axis in the midplane. This injection angle can be attained by installing a NBI parallel to the shield. For reference is shown the angle of 30° attained by a line passing through the point B and the normal to the plasma axis in the midplane. Angles shown in other cases (N=8,10,16) are determined in the same way. The point B for N=8, 10 and 16 is set at the same distance from TF coils as for N=12. Except for the case of N=16 the position of the shield 1.0 m thick is located at the same distance from the toroidal axis as that for N=12. The 1.0 m shield for N=16 is placed at a 10 cm distance from TF coils as well as the 0.8 m shield.

These figures are provided to have a dimensional understanding of the TF coils size and the allowable NBI port size for discussion on an interrelation among the number of TF coils, the beam injection angle, the space required for shield, blanket, coolant pipes, repair and maintenance and poloidal coil configuration.

3. Ripple loss of fast ions during slowing down

3.1 Model

The ripple produced by the finite number of toroidal field coils results in local magnetic mirrors between the coils. High energy ions trapped in the ripple well drift vertically to the wall and will be lost directly from the plasma without contributing to plasma heating.

We have investigated the effect of toroidal field ripple on the loss of fast ions produced from neutral beam injection for the INTOR parameters suggested for Phase I⁽¹⁾. The parameters used are listed in Table 1. The number (N) of TF coils considered is 8, 10, 12 and 16. An emphasis is placed on the case of N=12. A parabolic distribution is assumed for the plasma temperature and current. The plasma density profile is set to be

$$n(r) = n_0 \left(1 - \left(\frac{r}{a}\right)^6\right) + n_s \quad (1)$$

based on the results of one-dimensional transport simulation⁽⁵⁾, while the previous report⁽⁶⁾ presented at the INTOR Workshop in March deals with a parabolic density profile.

The form taken for the spatial distribution of toroidal field ripple is

$$\left. \begin{aligned} \delta &= \delta_0 \delta_1(r) \exp(-\beta\theta^2) \\ \delta_1(r) &= \left(\frac{r}{a}\right)^2, \quad \delta_0 = \frac{B_{\max} - B_{\min}}{B_{\max} + B_{\min}} \end{aligned} \right\} \quad (2)$$

where θ is poloidal angle. In the present analysis $\beta = 0.5$ is employed. The δ_0 -value is defined at the outer edge of the plasma and covers a range of 0.4~1.0 % for survey calculations.

The detailed behaviours of fast ions during slowing down process in a non-axisymmetric magnetic field have been analyzed with a Monte-Carlo simulation technique⁽²⁾. The Monte-Carlo technique is adopted to simulate the following collisional processes;

- i) Coulomb collision of fast ions with plasma ions and electrons with the Maxwellian velocity distribution.
- ii) Coulomb collision of fast ions with impurity ions.

Charge-exchange reactions are excluded in the present calculation.

Calculations of these collisional processes have been carried out for every test particle drifting along their guiding center orbits, which is described by

$$\frac{dv_{g\parallel}}{dt} = -\frac{\mu}{m} \frac{\partial B}{\partial \ell}, \quad \vec{v}_{g\perp} = -\frac{v_{\parallel}^2 + v_{\perp}^2/2}{\Omega} \vec{b} \times \frac{\partial \vec{b}}{\partial \ell} \quad (3)$$

where μ is the magnetic moment, $\vec{b} = \vec{B}/|B|$ and $\Omega = -qB/m$.

The magnetic field B is given by

$$\left. \begin{aligned} \vec{B} &= \vec{B}_{\psi}(r, \theta, \psi) + \vec{B}_{\theta}(r, \theta) \\ B_{\psi} &= B_t(R_0/R)(1 + \delta \cos N\psi) \quad (\text{toroidal magnetic field}), \\ B_{\theta} &= (R_0/R)B_p(r) \quad (\text{poloidal magnetic field}), \end{aligned} \right\} (4)$$

B_t : toroidal field on the magnetic axis (R_0),

B_p : poloidal field defined by the plasma current,

N : number of the toroidal field coils,

The plasma shape is circular. The birth profile of ions is given by an approximation of pencil beam injection.

3.2 Results

Fast ions are lost through two kinds of processes. (1) ripple-trapped drift loss and (2) banana drift loss. The energy fractions lost to the wall are shown in Figs.3~5 as a function of injection angle or ripple for coinjection, where G_{rt} is the energy loss due to ripple-trapped drift motion, and G_t is a sum of G_{rt} and G_{ro} , the loss due to banana drift motion. The injection angle φ is defined as an angle produced between the beam line and a normal to the plasma axis in the midplane. The value of G_{ro} includes the loss resulting from the ripple-enhanced banana drift and the detrapping from the ripple well. The energy loss comes mainly from the ripple-enhanced banana drift. The losses depend strongly on the ripple magnitude.

Figures 3 and 4 show the results for the plasma parameters at an termination of NBI heating which are set to be the ignited INTOR plasma parameters, i.e., $\bar{n} = 1.3 \times 10^{20} \text{ m}^{-3}$ ($n_s = 3 \times 10^{18} \text{ m}^{-3}$) and $\bar{T} = 10 \text{ keV}$ ($T_s = 0.3 \text{ keV}$) for average plasma density and temperature,

respectively. In Fig.4 the results for $N=8$ ($\delta_0 = 1.0\%$) and $N=16$ ($\delta_0 = 0.4\%$) are compared with those for $N=12$ with the corresponding δ_0 -values. We see in the figure that for the same ripple value increasing the number of TF coils results in an enhancement of the energy losses. The influence of N on G_{rt} is larger than on G_t . The higher plasma density and flatter profile than the previous case⁽⁶⁾ bring about substantial energy losses. In case of $\delta_0 = 0.75\%$ for $N=12$, for example, the loss fraction of the beam power is around 10% for $\varphi = 30^\circ$ and as high as $\sim 20\%$ for $\varphi = 20^\circ$.

The energy loss due to ripple-trapped particles results in a local heat deposit on the first wall. It should be noted that the G_{rt} -values obtained from the present Monte-Carlo calculation have large uncertainties, particularly for values lower than a few %. From the point of view of the countermeasure for a local heat load the cases for G_{rt} -values higher than a few % would be important. On each wall between TF coils the area of the heat load higher than 1% of the peak value is within about 1 m^2 , and typically $0.5\sim 1\text{ m}^2$ for G_{rt} higher than 3%. For a 75 MW injection power the average heat flux is less than 100 W/cm^2 , and typically $50\sim 100\text{ W/cm}^2$ for G_{rt} higher than 3%. The peak heat flux is typically $\sim 200\text{ W/cm}^2$, though a magnitude of $\sim 400\text{ W/cm}^2$ appears in some cases, e.g., for $N=12$, $\delta_0 = 0.75\%$ and $\varphi = 15^\circ$. In case of heat load higher than 5% of the peak value, the heat-deposit wall area reduces by 20~40%, and consequently the average heat flux increases by the corresponding factors.

Figure 5 illustrates variations of the energy losses with time during the NBI heating phase where the heating is assumed to start at t_s and terminate at t_f , and t_h represents an intermediate time point between t_s and t_f . The average plasma density and temperature at each time are shown in the figure. T_s at t_s is 0.1 keV. The density profile at t_s is assumed to be parabolic, while considering a flat profile due to external additional fueling the profile at t_h is set to be $[1 - (r/a)^6]$ as well as at t_f .

The required NBI power capacity is determined by the maximum energy loss which occurs at t_f . On the other hand the countermeasures for the protection of the first wall depend on the magnitude of heat flux, its distribution and heating duration. For a heating pulse length of some 5 seconds usually employed the time-integrated heat load would be important in connection with thermal properties of the

protection material used. The heat load estimated at t_h would give a measure as an average.

It is difficult to simulate the noncircular INTOR plasma with the present Monte Carlo code. In fact there is a large difference in many characteristics between the circular model and the INTOR plasma. Major problems would come from differences in plasma current (poloidal field configuration also) and ripple configuration. Setting the same safety factor in a circular plasma as in a non-circular plasma results in a substantial decrease of plasma current. Raising the plasma current up to the value in the non-circular plasma considerably improves the confinement of suprathreshold ions. On the other hand, in the non-circular plasma ripple variations along magnetic surfaces in the poloidal direction are moderate compared with in the circular plasma. Changing β -value of 0.5 to 0.2 we exemplify the effect of poloidal variation of ripple on the energy loss. For $N=12$ and $\delta_0 = 0.75\%$, for example, the loss fraction of G_{rt} increases about twice and G_t does by 20~30 % for $\varphi = 20\sim 30^\circ$. Of course we could not properly simulate the ripple well configuration for a non-circular plasma by using β -value alone. It should be noted that in the model used the magnetic axis coincides with the plasma axis centered at the major radius.

Anyway, to determine definitely the NBI energy loss for the INTOR plasma we should develop a Monte Carlo orbit-following calculation code capable of treating a non-circular plasma. In that case an MHD equilibrium analysis should be incorporated to consider the magnetic flux surface configuration particularly for a high β -plasma which is considerably different from the present model. Finally we should note a rather optimistic assumption made for beam species. The energy components of the neutral beam used (see Table 1) come from the fraction of extracted ion species of $D^+:D_2^+:D_3^+ = 90:7:3$, which is set as a target of R and D for an ion source by the INTOR construction phase⁽⁷⁾. If this high fraction of monoatomic beam is not attained, the ion energy loss will increase due to the increase of lower energy beam species trapped near the plasma boundary.

Further analysis and investigation of these matters are required.

4. Toroidal field ripple required to achieve a stable plasma burning

According to the experiments of the present-day tokamaks, electron energy confinement obeys the empirical scaling law (Alcator scaling law), and the ion thermal conductivity is almost 3 times neo-classical value. The electron thermal conductivity is independent of temperature and the temperature dependence of ion thermal conductivity is favorable in view of confinement, so that the plasma will make a thermal excursion once the ignition is reached.

At present, one of the most promising methods to suppress the thermal excursion and to achieve a stable burning is one using variable toroidal field ripple^{(1)(8)~(10)}. In this section, we will evaluate the required value of toroidal field ripple to achieve a stable plasma burning by using one-dimensional tokamak transport code⁽³⁾.

This code treats deuterium, tritium, fast α particles and ash helium particles separately. The transport model is based on the INTOR guiding model;

$$\chi_e = \frac{5 \times 10^{19}}{n_e(r)} f(\kappa) \quad (\text{m}^2/\text{s}) \quad , \quad (5)$$

$$\chi_i = [3(\chi_i)_{nc} + \chi_r] f(\kappa) \quad , \quad (6)$$

$$D = \frac{\chi_e}{12} \quad , \quad (7)$$

where κ is ellipticity. The transport code simulates a circular cross section plasma, while the actual plasma shape is noncircular. Thus we modify transport coefficients by a factor of $f(\kappa) = \frac{\sqrt{1+\kappa^2}}{2}/\kappa$, which represents the volume-surface ratio. This way of modification is more reasonable than employing a larger minor radius $a_{\text{eff}} = a\sqrt{\kappa}$, since in the latter the volume-surface ratio is not taken into account correctly and the heat deposition profile of neutral beam injection is altered. The expression of ion thermal conductivity due to toroidal field ripple χ_r is given as⁽¹¹⁾

$$\chi_r = 46.5 \frac{G(\alpha, \beta; \sigma) \delta_0^{3/2}(r)}{v_{ii}} \left(\frac{T_i}{eBR} \right)^2 n_i, \quad (8)$$

where δ_0 is the magnitude of peak-to-average ripple value and $G(\alpha, \beta; \sigma)$ is some complicated function. A simplified form of G is given in Ref.(11). However to evaluate the ripple effect correctly, the non-circularity of the plasma shape and the poloidal angle (θ) dependence of the ripple structure must be carefully taken into account⁽¹²⁾. Thus we incorporate the expression for G given in Ref.(12) into the tokamak code, and calculate G at each time step. The poloidal angle dependence of the ripple structure is assumed to be an exponential type as

$$\delta(r, \theta) \propto \delta_0(r) \exp(-\beta\theta^2) \quad (9)$$

We set $\beta = 0.5$. The effect of plasma elongation is represented by σ , for which we set $\sigma = 1.6$. α is a usual parameter; $\alpha(r) = \varepsilon / Nq \delta_0(r)$.

Using these transport models, we evaluate the required value of toroidal field ripple to sustain the plasma burning near the target temperature. In the neutral beam injection phase, the toroidal field ripple must be kept low to suppress the ripple loss of fast ions. The ripple value should be rapidly raised from the base value to the desired one once the ignition state is reached. After attaining the target temperature, the ripple value is changed slowly to realize a stable burning at that temperature. This is the typical scenario of burning control by toroidal field ripple.

We use the following model of toroidal field ripple δ .

$$\delta = S(t) \left\{ \delta_p + (\delta_a - \delta_p) \left(\frac{r}{a} \right)^2 \exp(-\beta\theta^2) \right\}, \quad (10)$$

$$S(t) = \left\{ \begin{array}{ll} 1 & t < t_0 \\ 1 + C \left\{ 1 - \exp\left(-\frac{t-t_0}{\tau}\right) \right\} & t \geq t_0 \end{array} \right\} \quad (11)$$

where δ_a : base ripple value at plasma surface, δ_p : base ripple value at plasma axis, β : poloidal dependence of ripple value, C : multiplication factor of variable ripple, t_0 : start time of raising ripple, τ : time constant of raising ripple. The toroidal field ripple is increased from its base value ($\delta_0 = 0.75\%$, $\delta_p = 0.035\%$) to the final

value which is set beforehand. When \bar{T}_i reaches about 10 keV, the final value of ripple is applied and simultaneously the NBI is turned off. Time constant of ripple rising, τ , is 1 second. Figure 6 shows the time behaviors of \bar{T}_i for various ripple values. When the magnitude of toroidal ripple is higher than the critical value, the ignition state cannot be sustained and the temperature falls down rapidly. From Fig.6, we conclude that the critical ripple magnitude is about 1.5 % at the outer edge of the plasma. Even if the ripple magnitude is within a critical value, gradual decreases of plasma temperature are observed in Fig.6. This is due to the helium ash accumulation and the flattening of fuel density profile⁽⁵⁾. To keep the burning temperature constant in time, further slow control of the ripple will be required⁽¹⁰⁾.

5. Discussion

Major physical issues determining the number and size of TF coils from the viewpoint of ripple are considered to be requirements for stable burning and beam ion confinement. The requirements from the two issues are contrary each other. Engineering measures for variable field ripple should be taken. For example, TF coils are designed to meet the acceptable ripple level for NBI heating, and after the NBI heating is turned off at ignition, variable ripple coils operate to raise the ripple up to the value required for burn control.

The number and size of TF coils are not decided by physical considerations alone. Major engineering issues which must be considered would be

- (1) Repair and maintenance
- (2) Magnet design issues including poloidal coils
- (3) Capacity of electric power and operation cost
- (4) Cost of magnet fabrication and a reactor system
- (5) Perspective of R and D.

For greater than 12 coils the space inside TF coils with $\delta_0 = 0.75\%$ would be too narrow to accommodate blanket, shield, divertor, coolant pipes and the room required for the insertion and move of remote handling machines. The shield thickness of 1 m shown in Fig.2 which is employed for INTOR-J is not satisfactory from the viewpoint of access (maximum dose rate outside the shield is larger than 100 mrem/h)⁽⁴⁾. Neutronics requires thickness of 20~30 cm further for suitable shielding⁽¹³⁾. As a result, if $\delta_0 = 0.75\%$ is imposed, the 16-coil system (6.7 m horizontally by 9.6 m vertically) employing poloidal divertors seems to have no credible solution from the viewpoint of available shield thickness and injection angle. For the 12-coils system the injection angle should be more than 25° to reduce the beam energy loss to around 10% or less.

It should be noted that the results obtained have uncertainties, particularly in estimate of the injected ion confinement. Recently the ripple-diffusion and -conduction coefficients significantly less than the previous theory⁽¹¹⁾ are reported by Tani et al.⁽²⁾. If these results should be applied, the ripple field configuration must be modified to enhance the conduction. We must emphasize further

theoretical and experimental studies on the ripple effects, and also a study improving the computation time and accuracy for the Monte Carlo techniques.

Acknowledgement

The authors wish to thank K. Sako for useful discussions on ripple-related engineering and H. Kishimoto for his helpful comments on the NBI simulation. They also thank H. Nishida for great assistance in performing numerous calculations.

theoretical and experimental studies on the ripple effects, and also a study improving the computation time and accuracy for the Monte Carlo techniques.

Acknowledgement

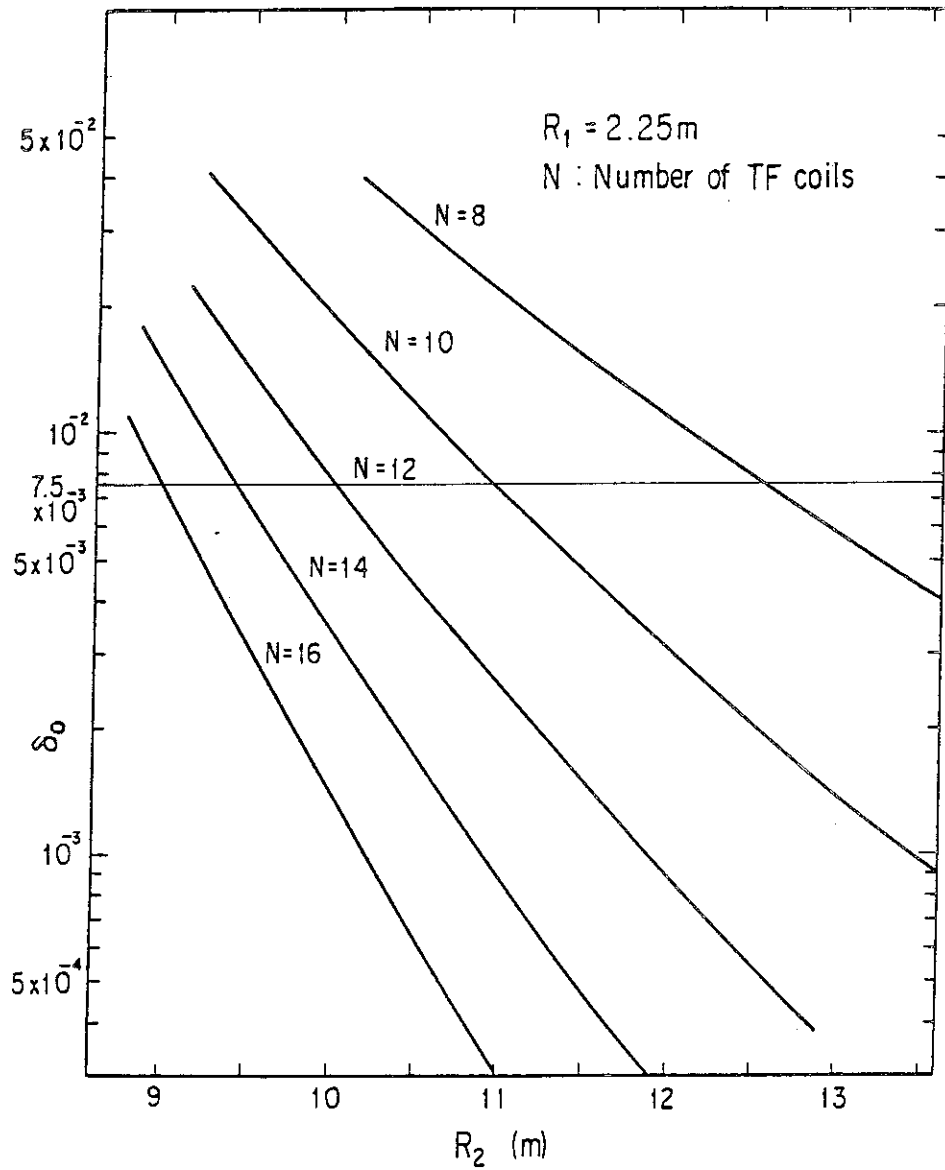
The authors wish to thank K. Sako for useful discussions on ripple-related engineering and H. Kishimoto for his helpful comments on the NBI simulation. They also thank H. Nishida for great assistance in performing numerous calculations.

References

- (1) INTOR Group: "International Tokamak Reactor", Nuclear Fusion, Vol.20, No.3, 349 (1980).
- (2) Tani, K., Kishimoto, H. Tamura, S.: 8th IAEA International Conference on Plasma Physics and Controlled Nuclear Fusion Research, Brussels, 1980, IAEA-CN-38/W-2-2.
- (3) Tone, T., Maki, K., Kasai, M.: To be published in a JAERI-M report.
- (4) Sako, K., Tone, T., Seki, Y., Iida, H., et al.: "Engineering Aspects of the JAERI Proposal for INTOR (II)", JAERI-M 8518 (1979).
- (5) Sugihara, M.(ed.): "IAEA INTOR Workshop Report, Group 1 — Energy and Particle Confinement —", JAERI-M 8621 (1980).
- (6) Tone, T., Yamamoto, T., Tani, K.: Report submitted to the IAEA INTOR Workshop in March, 1980.
- (7) Shirakata, H.(ed.): "IAEA INTOR Workshop Report, Group 4 — Heating —", JAERI-M 8623 (1980).
- (8) Tone, T.(ed.): "IAEA INTOR Workshop Report, Group 12 — Start-up, Burn and Shutdown —", JAERI-M 8625 (1980).
- (9) Petrie T.W., Rawls J.M.: Nuclear Fusion 20 (1980) 419.
- (10) Sugihara M. et al.: submitted to J. Nucl. Sci. Tech..
- (11) Connor J.W., Hastie R.J.: Nuclear Fusion 13 (1973) 221.
- (12) Uckan N.A. et al.: ORNL/TM-5603 (1976).
- (13) Seki, Y.: Private communication.

Table 1 Plasma and neutral beam parameters

major radius	$R = 5.2$ (m)
minor radius	$a = 1.3$ (m)
toroidal field	$B_t = 5.5$ (T)
temperatures	$T_e(r) = T_i(r) = T_0(1 - (r/a)^2) + T_s$ (eV) $(T_D(r) = T_T(r) = T_i(r))$
plasma density	$n_e(r) = n_0(1 - (r/a)^m) + n_s$ (m^{-3}) $(n_D(r) = n_T(r) = n_i(r))$
plasma current	$j_p(r) = j_0(1 - (r/a)^2)$
safety factor	$q_a = 2.5$
effective Z	$Z_{eff} = 1.5$ (uniform)
charge number of impurity ion	$Z_{imp} = 8.0$ (oxygen)
beam energy	$E_b = 175$ (keV)
beam power	75 MW
power ratio of neutral beam components	$E_b : E_b/2 : E_b/3 = 75 : 16 : 9$
toroidal field ripple	$\delta = \delta_0 \delta_1(r) \exp(-\beta\theta^2)$, $\delta_1(r) = (r/a)^2$
number of toroidal coils	$N_t = 8, 10, 12, 16$



Toroidal field ripple at the outer edge of the INTOR plasma

Fig.1 Toroidal field ripple at the outer edge of the plasma for constant tension D-shaped coils.

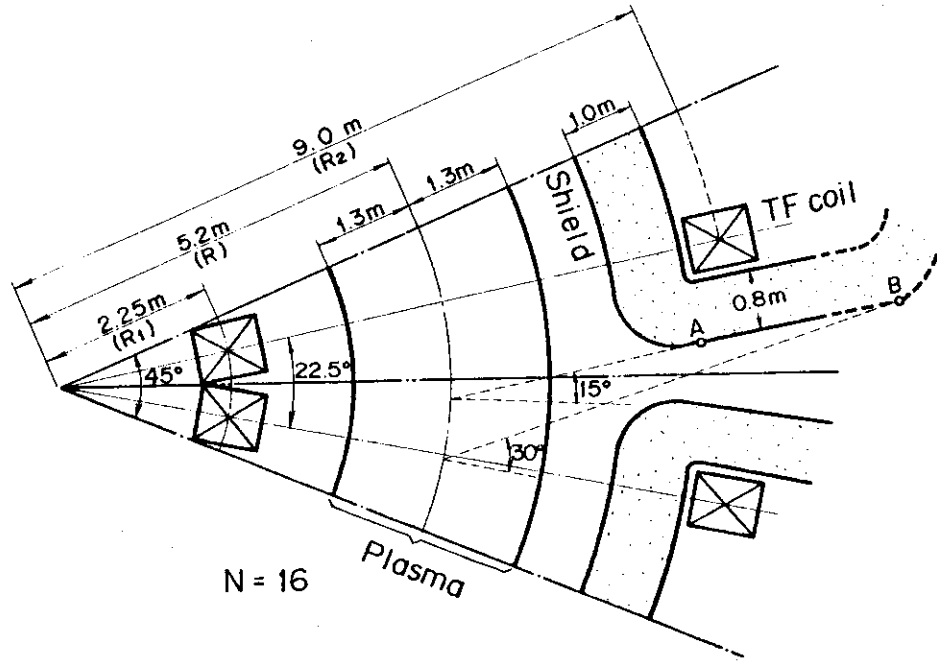


Fig. 2 (a) N=16;

Fig. 2 Horizontal cross section of the torus in the midplane. The toroidal-coils configuration gives a $\pm 0.75\%$ ripple at the outer edge of the plasma.

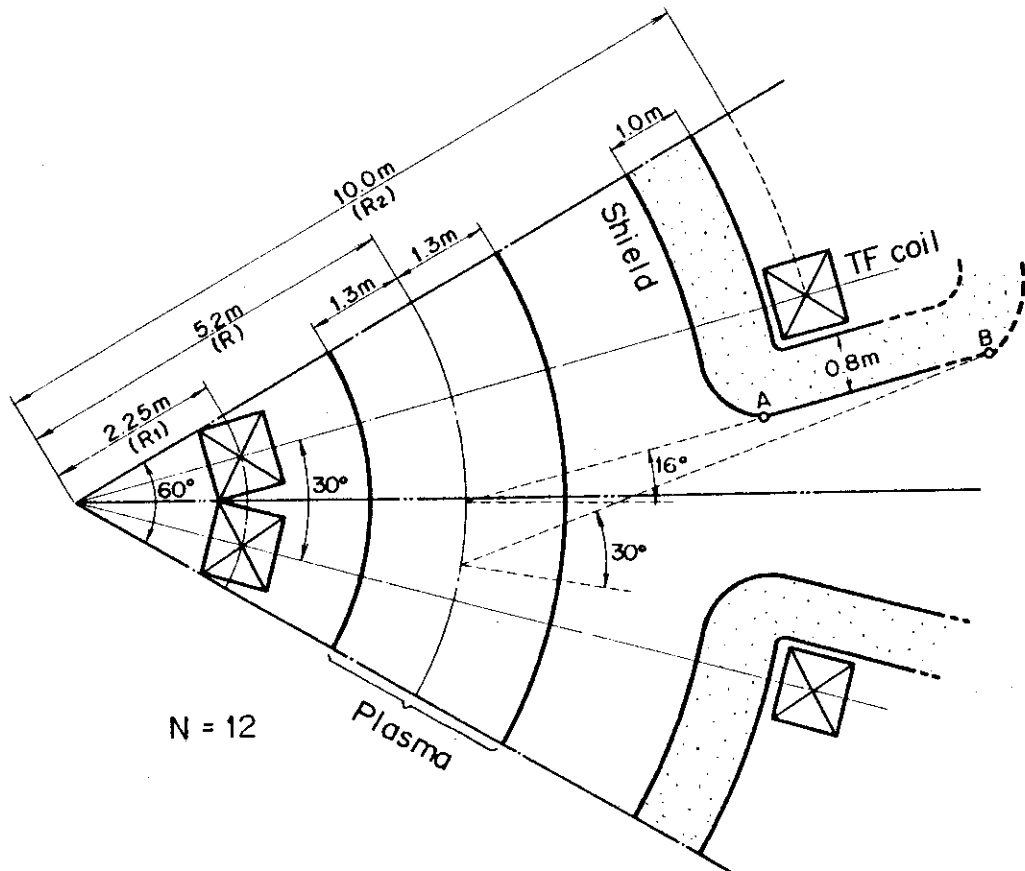


Fig. 2 (b) N=12;

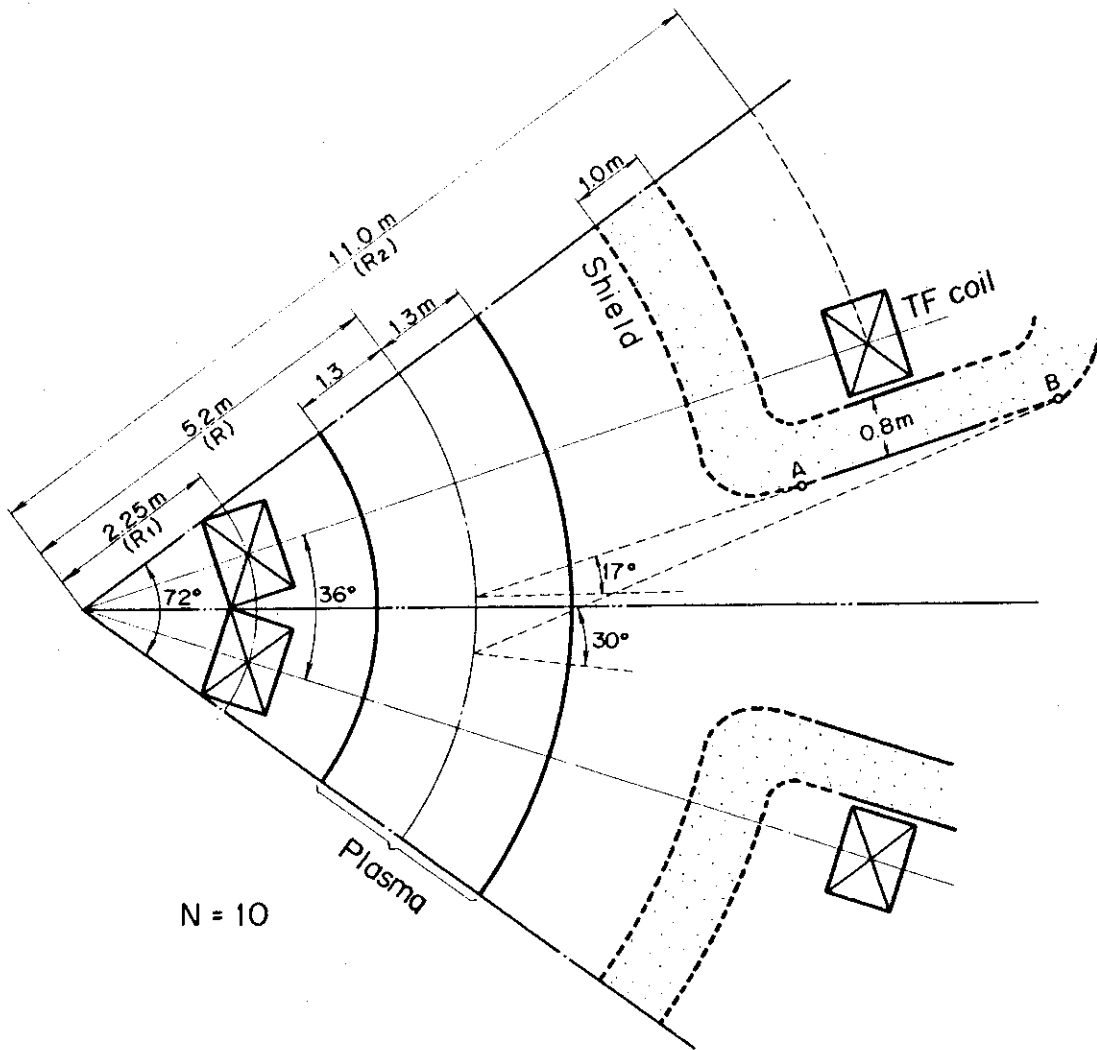


Fig. 2 (c) $N = 10$;

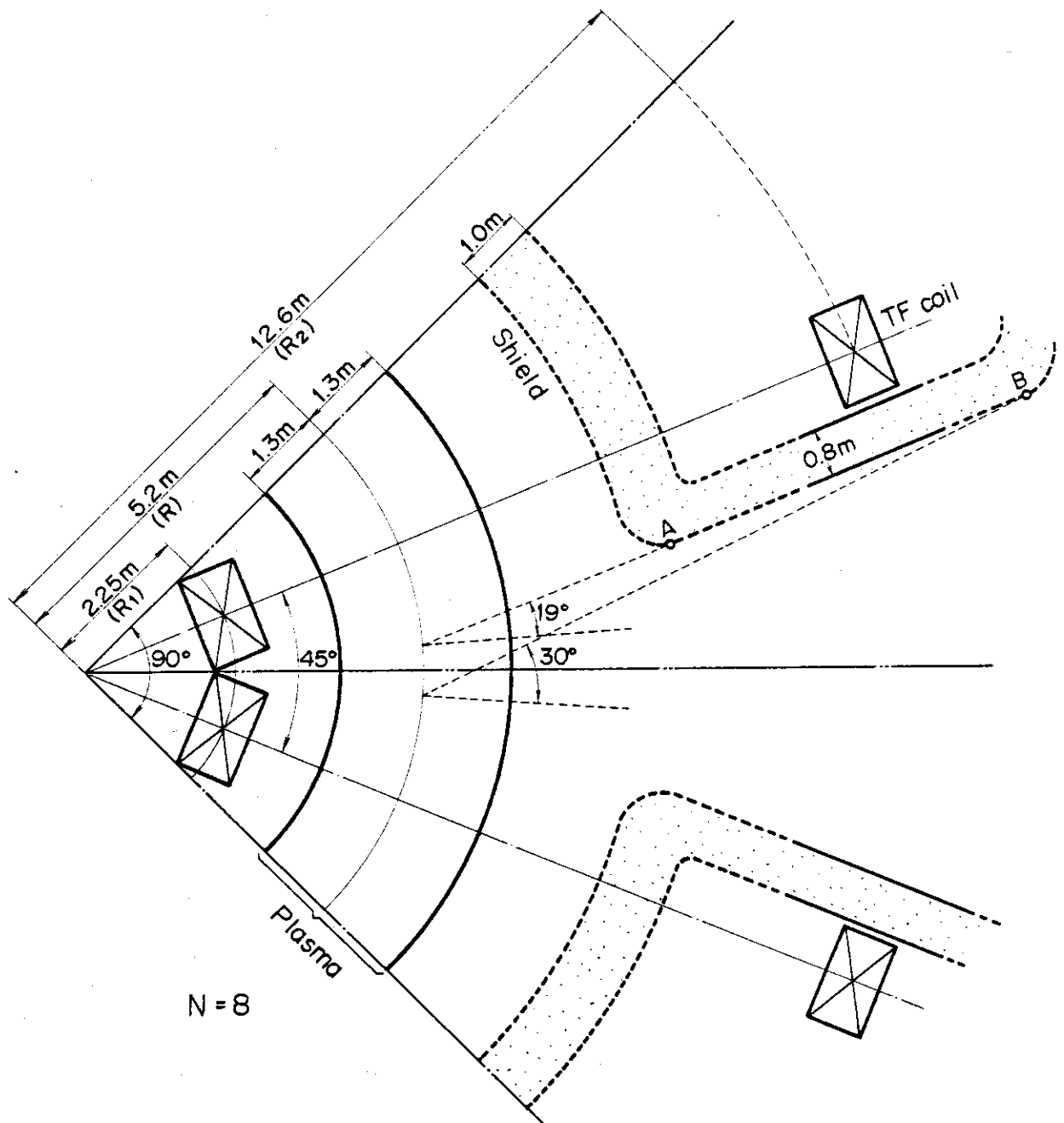


Fig. 2 (d) $N=8$.

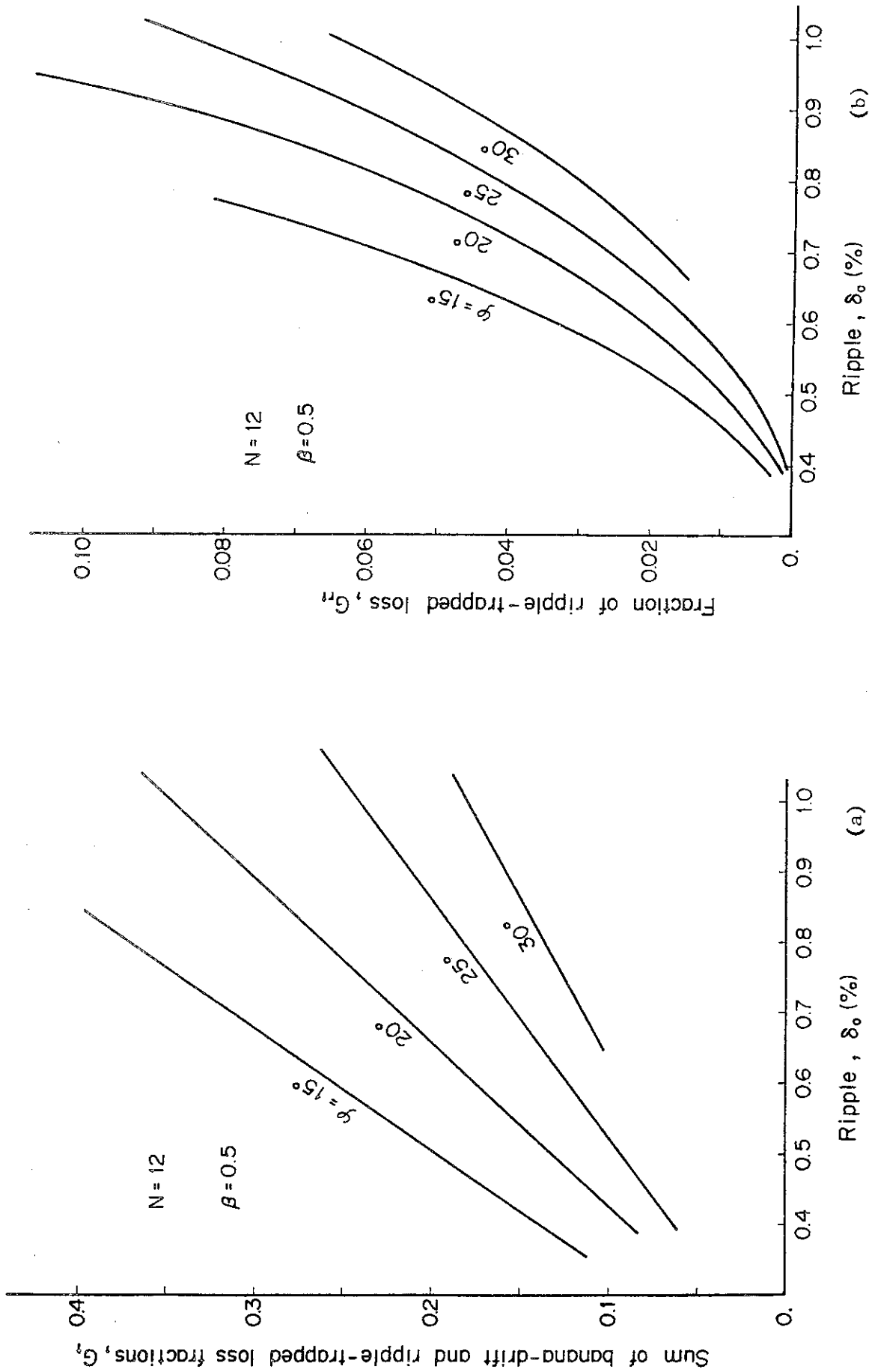


Fig.3 Fraction of beam energy loss for $N=12$

(a) sum of banana-drift and ripple-trapped losses;

(b) ripple-trapped loss.

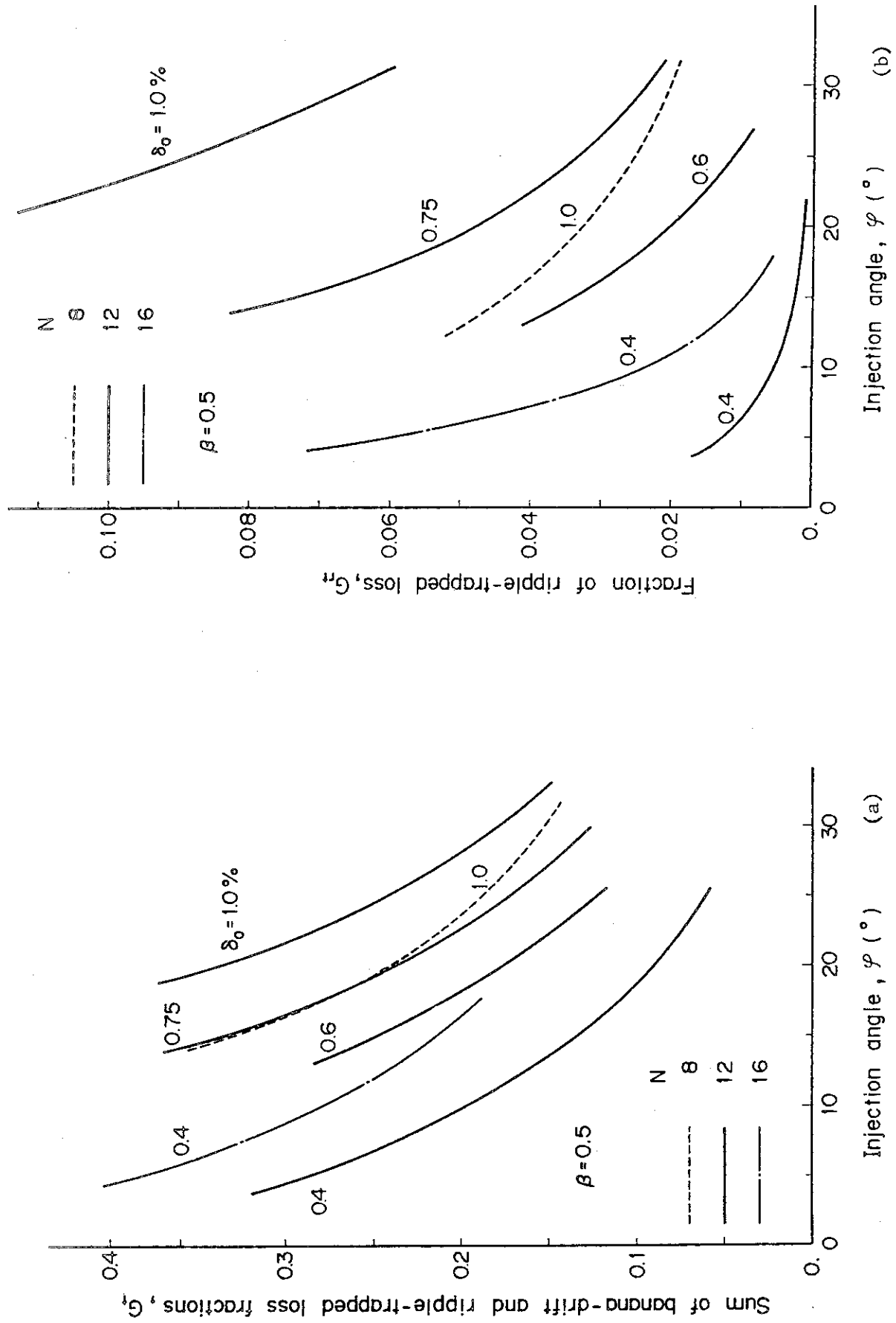


Fig.4 Comparison of beam energy loss for various TF-coil numbers

(a) sum of banana-drift and ripple-trapped losses;

(b) ripple-trapped loss.

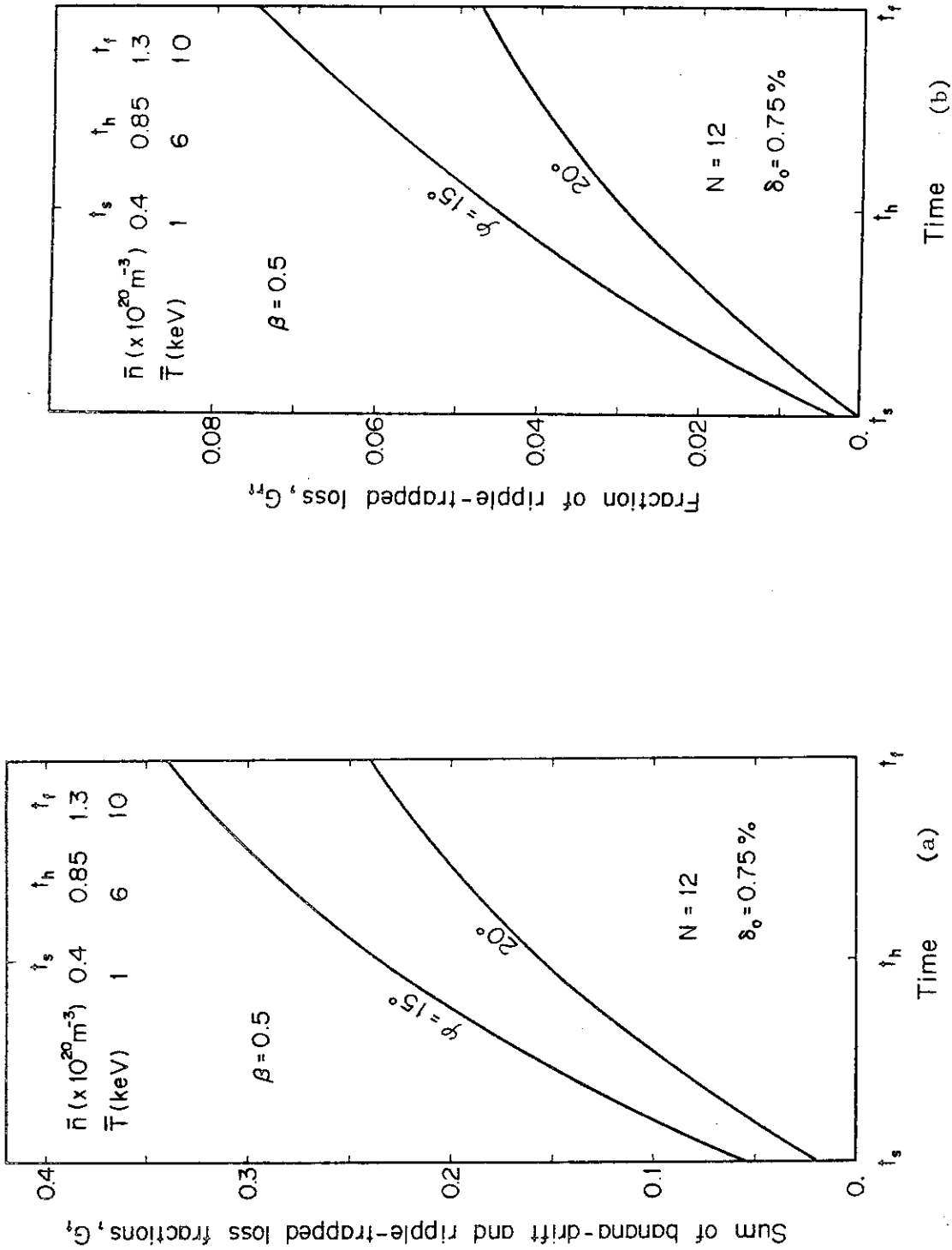


Fig.5 Variation of beam energy loss during NBI heating phase

(a) sum of banana-drift and ripple-trapped losses;

(b) ripple-trapped loss.

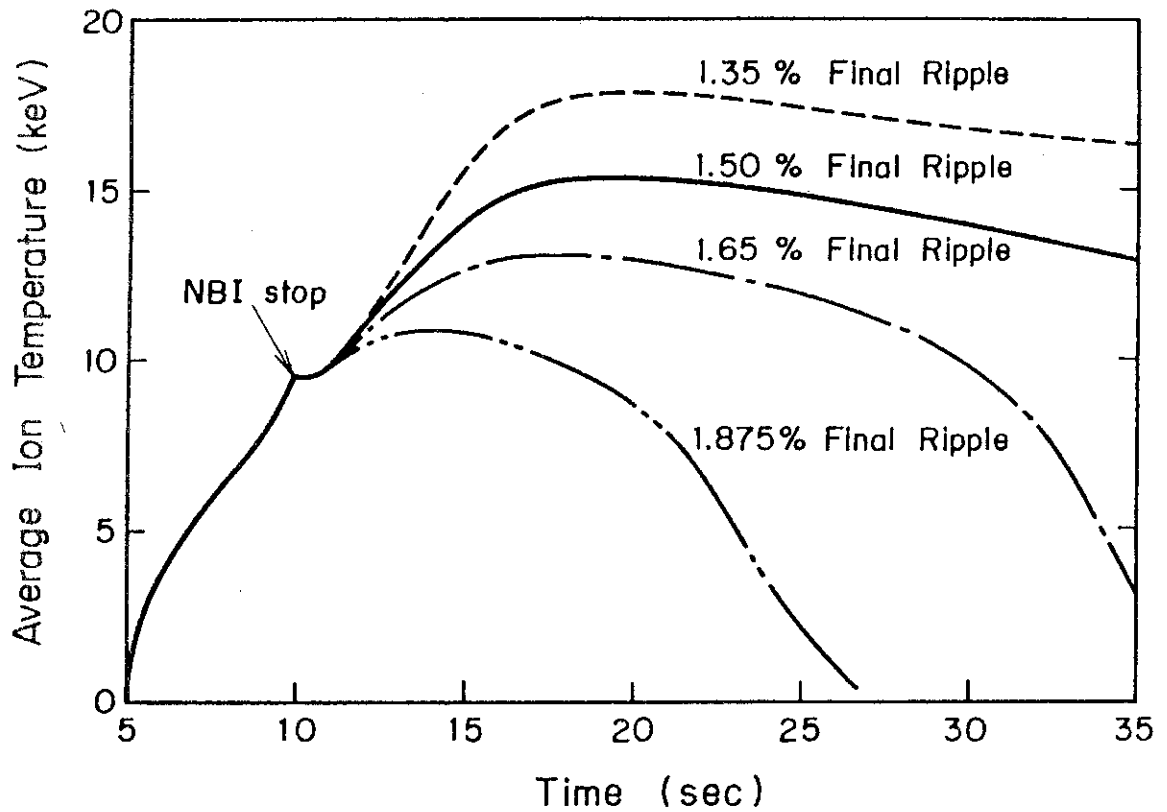


Fig.6 Time behavior of average ion temperature for various final ripple values at the plasma surface. NBI is turned off at $\bar{T}_i \sim 10$ keV. Stable plasma burning is obtained within a critical beta value for $\delta_0 \sim 1.5$ %.